

Tailoring the magnetic order in a supermagnetic metamaterial

Sam D. Sløetjes,^a Hans Henrik Urdahl, Jostein K. Grepstad, and Erik Folven
Department of Electronics and Telecommunications, Norwegian University of Science and Technology, O.S. Bragstadsp. 2A, NO-7491 Trondheim, Norway

(Presented 2 November 2016; received 23 September 2016; accepted 26 November 2016; published online 6 March 2017)

The emergent magnetism in close-packed assemblies of interacting superparamagnetic particles is commonly referred to as supermagnetism. The magnetic characteristics of such systems are determined by the dipolar coupling between the nanomagnets, rather than the exchange interaction responsible for ferro- and antiferromagnetism in continuous material. The dipolar coupling facilitates tuning of the magnetism, which renders supermagnetic ensembles suitable model systems for exploration of new physics. In this work, we discuss micromagnetic simulations of regular arrays of thin film nanomagnets, with magnetic material parameters typical of the ferromagnetic oxide $\text{La}_{0.7}\text{Sr}_{0.3}\text{MnO}_3$. The ground state supermagnetic order in these systems is primarily determined by the lattice configuration, in that a square lattice results in antiferromagnetic order, whereas a triangular lattice shows ferromagnetic order. We found that a square lattice of circular nanomagnets may be switched from superferromagnetic to superantiferromagnetic order by a small external field applied in the appropriate direction. © 2017 Author(s). All article content, except where otherwise noted, is licensed under a Creative Commons Attribution (CC BY) license (<http://creativecommons.org/licenses/by/4.0/>). [<http://dx.doi.org/10.1063/1.4978319>]

Novel materials with enhanced magnetic properties are important to industries ranging from automotive to microelectronics. Assembly of nanoparticles offers an interesting approach to the design of new magnetic materials and devices, such as permanent magnets for electric cars,¹ spintronic memory and magnetic logic that may form the basis for ultra-low energy computing,² soft magnetic materials for high frequency magnetic sensors,³ and biomedical technology for hyperthermia treatment.⁴ Moreover, arrays of nanomagnets may serve as model systems to explore new fundamental physics, such as emergent magnetic monopoles⁵ and magnetic frustration in 2-dimensional (2D) artificial spin ice systems.⁶

The emergent magnetism in ensembles of interacting nanomagnets that would be superparamagnetic if decoupled is referred to as supermagnetism.⁷ In such assemblies, the individual nanomagnets behave as superspins, i.e., magnetic moments orders of magnitude larger than atomic moments. The long-range order in such arrays is due to dipolar coupling between the individual nanomagnets (Figure 1), in contrast to the case for a continuous ferromagnet where the magnetic order is determined by exchange interaction. By varying size, shape, geometric arrangement, and spacing of the individual single-domain nanomagnets the strength and sign of the dipolar interaction, favoring either parallel (ferromagnetic) or antiparallel (antiferromagnetic) orientation of the moments in adjacent magnets, can be tuned and lead to new magnetic phenomena.^{8,9} Thus, supermagnetism offer a new avenue for design and control in nanoscale magnetic materials and devices, provided the collective magnetic properties can be controlled at the nanoparticle level.

Experimental studies of supermagnetism are scarce, presumably due to demanding fabrication and limited options for verification of the magnetic behavior in such systems.¹⁰

^aCorresponding author. E-mail: sam.sloetjes@ntnu.no

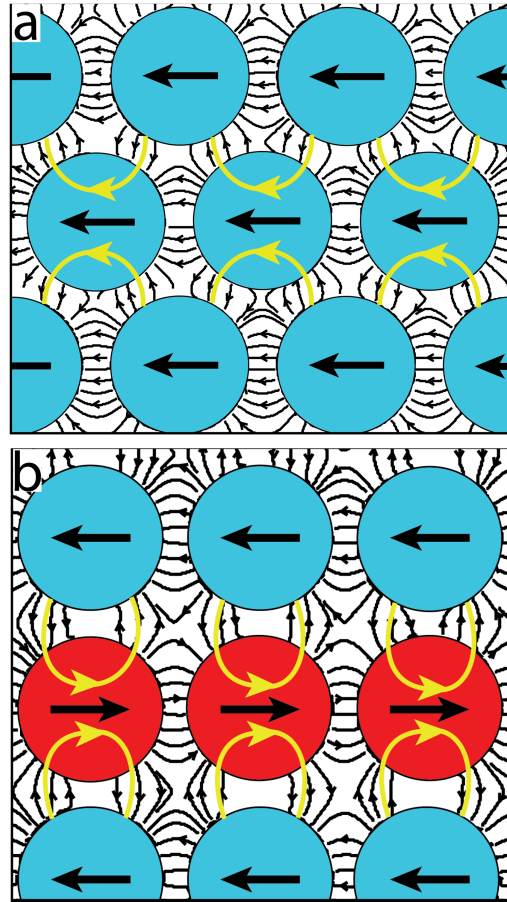


FIG. 1. The emergence of a) superferromagnetic and b) superantiferromagnetic order through dipolar coupling.

However, with modern thin film fabrication tools and advanced imaging techniques capable of probing magnetism in the sub-100 nm regime, this is set to change. The long-range order in regular lattices of magnetic dipoles has already been the subject of extensive theoretical inquiry. Most theoretical work on supermagnetism, more specifically on dipolar-coupled magnetic lattices, treat regular arrays with a well-defined lattice symmetry,^{11–14} where the individual dipolar-coupled nanomagnets are assumed to be monodomain.¹⁵

In the present study, we explore supermagnetism in arrays of 5 nm thick circular nanomagnets using the micromagnetic simulation software MuMax3.¹⁶ This is an open-source GPU-accelerated code that solves the Landau-Lifshitz equation.¹⁷ Our model system is $\text{La}_{0.7}\text{Sr}_{0.3}\text{MnO}_3$ (LSMO), a ferromagnet with a cubic magnetocrystalline anisotropy.¹⁸ The material parameters adopted in the present simulation were an exchange stiffness of $A_{\text{ex}} = 1.7\text{e-}12$ J/m, a saturation magnetization of $M_{\text{s}} = 4.5\text{e}5$ A/m, and a cubic magnetocrystalline anisotropy constant of $K_{\text{c}1} = 100$ J/m³. In order to ensure mesh independence, the discretization cell dimensions were set smaller than the exchange length $l_{\text{ex}} = \sqrt{2A_{\text{ex}}/\mu_0 M_{\text{s}}^2}$, which comes to approximately 4.7 nm for the set of magnetic parameters quoted. Mesh independence also requires that the edges of the nanomagnet are sufficiently smooth. For this reason, an upper bound of 2 nm was adopted for the in-plane cell size. The out-of-plane dimension was set equal to the disc thickness of 5 nm. All simulations were performed at zero Kelvin, and the damping parameter was set to $\alpha = 1$.

Prior to simulating arrays, we made an assessment of the diameter for which the individual circular nanomagnets exhibit a monodomain magnetic ground state, a prerequisite for superparamagnetic

behavior. To this end, the magnetic ground state of nanomagnets with diameters ranging from 20 nm to 140 nm were investigated. Because of their small thickness compared to the in-plane dimensions, shape anisotropy rendered the magnetization in the nanomagnets effectively 2D. The magnetic ground state was found by letting the system relax to its minimum free energy from a random initial magnetization state. This procedure was repeated 50 times for each nanomagnet diameter.

The two magnetic ground states emerging from these simulations were a monodomain state and a vortex state, as depicted in Figure 2. If the average reduced magnetization of the nanomagnet was larger than $|\langle \mathbf{m} \rangle| \geq 0.95$, it was regarded to be monodomain. In order to assess the relative stability of these two magnetic ground states, we plotted their free energy density versus the disc diameter, as shown in Figure 2. For disc diameters smaller than 60 nm the simulations invariably led to a monodomain ground state. This outcome results from predominance of the magnetic exchange interaction at this length scale. For disc diameters larger than approximately 90 nm, on the other hand, a vortex ground state was found to be energetically favorable. At these diameters the formation of a vortex state gives rise to a reduction in demagnetization energy larger than the penalty paid in increased exchange energy. Based on this result, we chose a diameter of 50 nm for individual elements of the nanomagnet arrays.

We investigated two different 2D arrays with triangular and square lattice symmetry, respectively, and a nearest-neighbor particle separation of 10 nm. These configurations have previously been shown to stabilize superferromagnetic (SFM) and superantiferromagnetic (SAF) ordering, respectively.⁸ Figure 1 shows how dipolar coupling gives rise to SFM and SAF ordering for the respective lattices. The simulated arrays were approximately $1.8 \times 1.8 \mu\text{m}^2$, with 34 rows of 30 magnets each for the triangular lattice and 30 rows of 30 magnets each for the square lattice. The discretization grid was set to 1024×1024 cells. We also note that the nanomagnet diameter and interparticle spacing in these simulations are within the manufacturing capability of modern thin film nanofabrication tools.

We first identified the magnetic ground state of the two arrays. To this end, we initialized the individual cells in the simulation mesh (not to be confused with the nanomagnets) with a random magnetization and let the system relax to a state of minimum free energy. This procedure was repeated 50 times for each array. A typical ground state obtained for the triangular array is shown in Figure 3a. We find SFM ordering with multiple domains several hundreds of nanometers across. While the domain state is reminiscent of that observed for a continuous ferromagnetic thin film,¹⁹ the characteristic domain size is significantly smaller. This is because the dipolar coupling, which favors parallel alignment of the nanomagnets in the array, is much weaker than the exchange interaction responsible for the spin alignment in a continuous ferromagnet. For this reason, shape effects in this

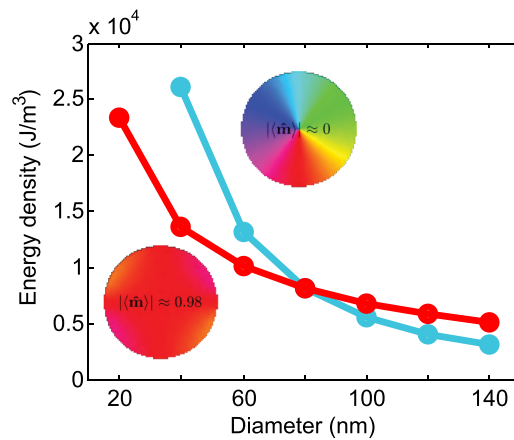


FIG. 2. The energy density of the vortex and monodomain ground states, plotted against nanomagnet diameter. The red curve represents the monodomain state, the blue curve represents the vortex state.

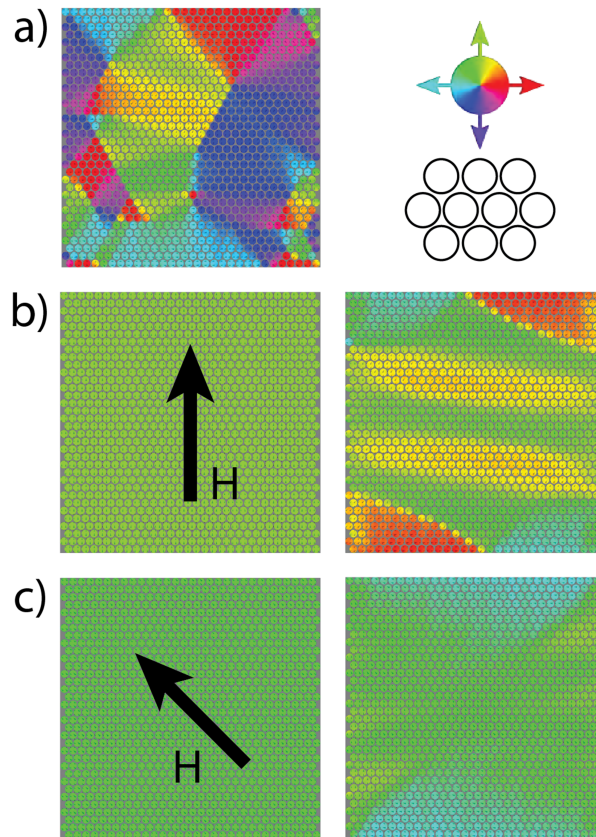


FIG. 3. Magnetization of the triangular array, a) in the absence of an applied magnetic field, b) saturated in a vertical direction (left) and then relaxed in the absence of a field (right), and c) saturated in a diagonal direction (left) and then relaxed in the absence of a field (right).

$1.8 \times 1.8 \mu\text{m}^2$ array are also less prominent than would be expected for a continuous micromagnet of comparable dimensions.²⁰

The same array of nanomagnets was simulated with a magnetic field applied in two different lattice directions. The arrays were first magnetically saturated by a field of 10 mT applied in the vertical (i.e., parallel to the array edge) and diagonal direction, respectively, as depicted in Figure 3b,c (left). The applied field was then removed, and the array was allowed to relax to its minimum free energy ground state, as shown in Figure 3b,c (right). In remanence, the vertically saturated array (Figure 3b) shows a multidomain SFM domain state with well-defined domain walls. The overall domain pattern has some resemblance with the “flower” state that was previously observed in simulations of blanket square nanomagnets.²¹ The array saturated along the diagonal (Figure 3c) shows a more or less homogenous magnetization without any abrupt domain walls.

Figure 4 shows results from simulations of arrays with a square lattice symmetry. Here, the supermagnetic order is distinctly different from the SFM ground state observed for the triangular lattice and can be described as a multidomain SAF state, cf. Figure 4a. The SAF domains are several hundred nanometers across and are seen to take on different shapes and sizes. This array was then saturated in a magnetic field of 10 mT applied along the vertical and diagonal direction, respectively. When subsequently allowed to relax to its minimum free energy ground state, the square array in Figure 4b,c (left) forms two distinctly different ground states in remanence, cf. Figure 4b,c (right). The vertically saturated array shows a predominant SAF ordering with two large domains oriented with their magnetic axis perpendicular to the direction of the initial applied field, see Figure 4b (right). The two domains are separated by a thin SFM domain aligned parallel to the initial applied field.

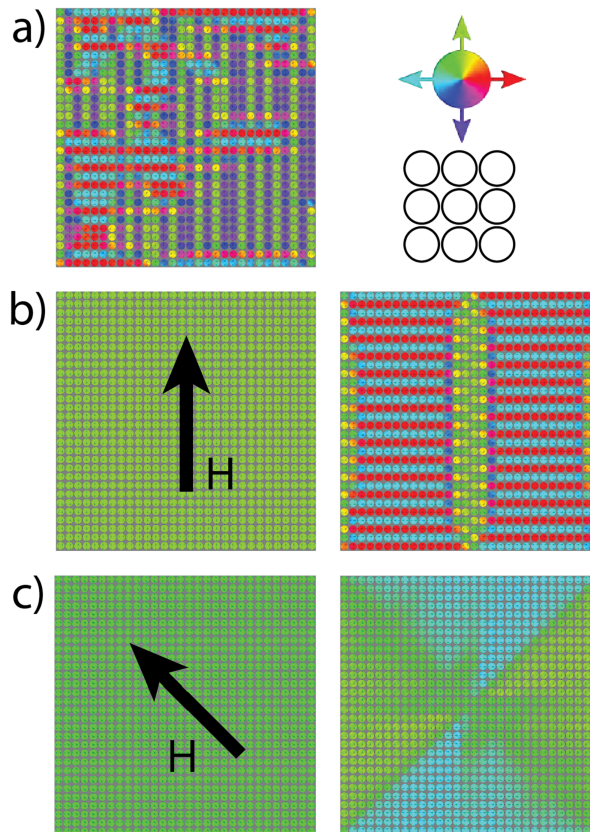


FIG. 4. Magnetization of the square array, a) in the absence of an applied magnetic field, b) saturated in a vertical direction (left) and then relaxed in the absence of a field (right), and c) saturated in a diagonal direction (left) and then relaxed in the absence of a field (right).

In contrast, the diagonally saturated array relaxes into a SFM ground state, resembling the ground state of the corresponding triangular array in remanence. These results suggest that a square array of nanomagnets can be switched in a controlled manner between SFM- and SAF-ordered magnetic ground states by application of an external magnetic field.

In summary, we have explored the emergent supermagnetic order in 2D arrays of LSMO nanomagnets using micromagnetic modelling. We find that monodomain nanomagnets arranged in a close-packed triangular lattice give rise to SFM long-range order with a domain pattern reflecting the 6-fold symmetry of the array, while SAF order emerges for nanomagnets arranged in a square lattice. Moreover, we found for the latter geometry that the supermagnetic long-range order can be switched from SAF to SFM using an applied magnetic field of a few mT. In contrast, switching the long-range order of a conventional antiferromagnet requires a magnetic field orders of magnitude larger, and the FM state would not persist in remanence. The difference is explained by the absence of exchange interaction between individual nanomagnets. The low switching field of this metamaterial between remanent states of predominant SAF and SFM order holds promise for future device applications as well as providing a test-bed for fundamental physics investigations.

ACKNOWLEDGMENTS

Partial funding for this work was obtained from the Norwegian PhD Network on Nanotechnology for Microsystems, which is sponsored by the Research Council of Norway, Division for Science, under contract no. 221860/F60.

- ¹ N. Jones, *Nature* **472**(7341), 22 (2011).
- ² R. Lavrijsen, J.-H. Lee, A. Fernández-Pacheco, D. C. Petit, R. Mansell, and R. P. Cowburn, *Nature* **493**(7434), 647 (2013).
- ³ S. Bedanta, T. Eimüller, W. Kleemann, J. Rhensius, F. Stromberg, E. Amaladass, S. Cardoso, and P. Freitas, *Physical Review Letters* **98**(17), 176601 (2007).
- ⁴ C. Martínez-Boubeta, K. Simeonidis, D. Serantes, I. Conde-Leborán, I. Kazakis, G. Stefanou, L. Peña, R. Galceran, L. Balcells, and C. Monty, *Advanced Functional Materials* **22**(17), 3737 (2012).
- ⁵ E. Mengotti, L. J. Heyderman, A. F. Rodríguez, F. Nolting, R. V. Hügli, and H.-B. Braun, *Nature Physics* **7**(1), 68 (2011).
- ⁶ A. Farhan, P. Derlet, A. Kleibert, A. Balan, R. Chopdekar, M. Wyss, L. Anghinolfi, F. Nolting, and L. Heyderman, *Nature Physics* **9**(6), 375 (2013).
- ⁷ S. Bedanta and W. Kleemann, *Journal of Physics D: Applied Physics* **42**(1), 013001 (2008).
- ⁸ M. Varón, M. Beleggia, T. Kasama, R. Harrison, R. Dunin-Borkowski, V. F. Puentes, and C. Frandsen, *Scientific Reports* **3** (2013).
- ⁹ M. Varón, M. Beleggia, J. Jordanovic, J. Schiøtz, T. Kasama, V. F. Puentes, and C. Frandsen, *Scientific Reports* **5** (2015).
- ¹⁰ R. López-Ruiz, F. Luis, J. Sésé, J. Bartolomé, C. Deranlot, and F. Petroff, *Europhysics Letters* **89**(6), 67011 (2010).
- ¹¹ V. Russier, *Journal of Applied Physics* **89**(2), 1287 (2001).
- ¹² P. Politi and M. G. Pini, *Physical Review B* **66**(21), 214414 (2002).
- ¹³ A. Fraerman and M. Sapozhnikov, *Journal of Magnetism and Magnetic Materials* **192**(1), 191 (1999).
- ¹⁴ V. Klymenko, V. Kukhtin, V. Ogenko, and V. Rosenbaum, *Physics Letters A* **150**(3), 213 (1990).
- ¹⁵ J. Jordanovic, M. Beleggia, J. Schiøtz, and C. Frandsen, *Journal of Applied Physics* **118**(4), 043901 (2015).
- ¹⁶ A. Vansteenkiste, J. Leliaert, M. Dvornik, M. Helsen, F. Garcia-Sanchez, and B. Van Waeyenberge, *AIP Advances* **4**(10), 107133 (2014).
- ¹⁷ L. D. Landau and E. Lifshitz, *Phys. Z. Sowjetunion* **8**(153), 101 (1935).
- ¹⁸ L. Berndt, V. Balbarin, and Y. Suzuki, *Applied Physics Letters* **77**(18), 2903 (2000).
- ¹⁹ R. M. Reeve, C. Mix, M. König, M. Foerster, G. Jakob, and M. Kläui, *Applied Physics Letters* **102**(12), 122407 (2013).
- ²⁰ Y. Takamura, E. Folven, J. B. R. Shu, K. R. Lukes, B. Li, A. Scholl, A. T. Young, S. T. Retterer, T. Tybell, and J. K. Grepstad, *Physical Review Letters* **111**(10), 107201 (2013).
- ²¹ R. Cowburn and M. Welland, *Physical Review B* **58**(14), 9217 (1998).